

## LETTER TO THE EDITOR

**Emission of correlated electrons from random alloys****Konstantin A Kouzakov and Jamal Berakdar**

Max-Planck-Institut für Mikrostrukturphysik, Weinberg 2, D-06120 Halle, Germany

E-mail: kouzakov@mpi-halle.de

Received 25 September 2002

Published 6 January 2003

Online at [stacks.iop.org/JPhysCM/15/L41](http://stacks.iop.org/JPhysCM/15/L41)**Abstract**

In this letter a theory is developed for the treatment of the ejection of two correlated electrons from binary alloys with substitutional disorder upon the impact of fast electrons. It is shown that, under certain conditions specified in this letter, the target's electronic properties can be disentangled from the correlated two-electron scattering. For a numerical realization we employ the Korringa–Kohn–Rostoker coherent potential approximation and the virtual crystal approximation for the description of respectively the bound states and the high-energy scattering states of the electrons. Numerical results are presented and analysed for the energy correlation within an electron pair emitted from a copper–nickel alloy surface.

**1. Introduction**

Since the early days of quantum mechanics electron beams have been employed to study a variety of material properties. For example the characteristic response of a solid surface can be probed by monitoring the probability for the energy  $E = \hbar\omega$  and the wavevector  $\mathbf{q}$  transfer to the target by a fast impinging electron [1]. Usually this method is utilized to study the frequency ( $\omega$ ) and the wavevector ( $\mathbf{q}$ ) behaviour of collective modes. On the other hand the incident electron beam may induce the emission of electrons with energy  $E$  and wavevector  $\mathbf{q}$ . For a detailed study of this channel one has to resolve at the same time the quantum numbers of the scattered and the emitted electrons. Such a measurement, referred to as the (e, 2e) experiment, has been successfully conducted on condensed matter targets in recent years [2–9]. Using a surface as a target the (e, 2e) experiment may be performed in two modes: (1) *the transmission* [3] (figure 1(a)) and (2) *the reflection* modes [2, 5] (figure 1(b)). In the transmission mode a valence-band electron is knocked out from the surface upon the passage of an energetic electron through a free-standing thin film. The scattered and the emitted electrons are detected in the forward direction with respect to the incoming beam. Since in this mode fast (compared to the Fermi velocity) vacuum electrons are involved the (e, 2e) process is well modelled by a direct, single collision between the projectile and the bound electron. In this case it has been demonstrated [10] that the (e, 2e) cross section is related directly to the

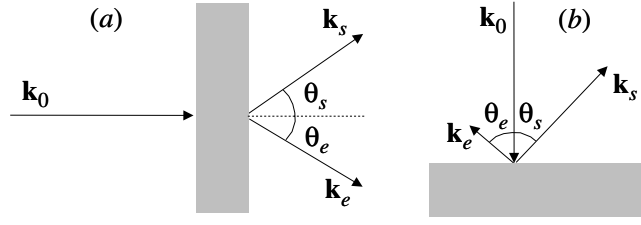


**Figure 1.** A sketch of the (e, 2e) process in (a) the transmission mode and (b) the reflection mode.

spectral properties of the (single quasi-particle) hole state. In the reflection mode all electrons propagate in the same half-plane (figure 1(b)), i.e. the emitted and the scattered electrons propagate in the direction opposite to the incident projectile. Therefore it is imperative to include in the theory, in addition to the electron–electron interaction, the scattering from the crystal potential [11]. In the reflection mode the energy of the electrons is low (0.5–500 eV) and one studies the dynamics of the electron–electron scattering at surfaces [8, 9, 12].

The (e, 2e) process has been studied theoretically and experimentally for a variety of ordered materials [2, 6, 7, 10, 12, 13]. First (e, 2e) experiments on alloys are presently in preparation. Therefore, it is timely to develop a theoretical framework for the investigation of the (e, 2e) process for disordered systems. This is done in this letter.

In the case of (e, 2e) from alloys one has to account for the effects of disorder on the scattering states of the correlated electron pairs as well as on the initially bound electronic state. As shown below, the structure of the (e, 2e) spectra are generally determined, in a non-trivial manner, by the properties of the initial and the final states as well as by the strength of disorder as quantified by the concentrations of the constituents of the alloy. Nevertheless, under certain conditions deduced below, one can achieve a decoupling of the scattering factors from initial state properties which, in this case, renders possible the use of (e, 2e) as a spectroscopic tool for the investigation of the electronic structure of alloys. Furthermore, to elucidate with numerical results the effect of disorder on the collision dynamics and examine the interplay between collisional effects and the target’s electronic structure we utilize the Korringa–Kohn–Rostoker coherent potential approximation (KKR CPA) [14–16] for the description of the ground state whereas the emitted (vacuum) electrons’ states are treated within the virtual crystal approximation (VCA). The numerical results are performed for the transmission and the reflection mode (e, 2e) from the surface of a copper–nickel alloy. Unless otherwise stated, atomic units (au) are used throughout.

## 2. General formulation

For a theoretical formulation we consider the (e, 2e) process in which, upon the impact of an electron with a wavevector  $k_0$  and energy  $E_0$  onto a solid surface, two electrons are emitted with wavevectors  $k_s, k_e$  and energies  $E_s, E_e$  (hereafter the subscript  $s$  ( $e$ ) refer to the scattered (ejected) electron). The fully differential (e, 2e) cross section is given by [11]

$$\frac{\sigma}{dE_s dE_e d\Omega_s d\Omega_e} = \frac{k_s k_e}{(2\pi)^5 k_0} \sum_{\substack{i_{occ} \\ s_s s_e}} | \langle k_{s s_s}, k_{e s_e} | T_{(e,2e)} | k_{0 s_0}, i s_i \rangle |^2 \delta(E_s + E_e - E_0 - \varepsilon_i). \quad (1)$$

The emission direction of the two final-state electrons are specified by the solid angles  $\Omega_{s(e)}$ . The final state of the two electrons having asymptotic wavevectors  $k_s, k_e$  and spin projections  $s_s, s_e$  is described by the correlated two-particle state  $|k_{s s_s}, k_{e s_e}\rangle$  which tends asymptotically

to  $|\mathbf{k}_s s_s\rangle \otimes |\mathbf{k}_e s_e\rangle$ . The initial state  $|\mathbf{k}_0 s_0, i s_i\rangle$  is a direct product of the projectile spinor state (with wavevector  $\mathbf{k}_0$  and spin  $s_0$ ) and a valence band state  $|i s_i\rangle$  with a spin projection  $s_i$ . The sum in (1) runs over the electrons' spin projections and over all occupied one-particle target states with energy  $\varepsilon_i = E_s + E_e - E_0$ .

The transition operator  $T_{(e,2e)}$  in the frozen-core approximation has the form [11]

$$T_{(e,2e)} = V_s + W_{se} + (V_s + V_e + W_{se})G_{se}^+(E_{\text{tot}})(V_s + W_{se}), \quad (2)$$

where  $V_s$ ,  $V_e$  and  $W_{se}$  are effective (optical) electron–solid and electron–electron scattering potentials, respectively.  $G_{se}^+(E_{\text{tot}})$  is the two-electron Green operator involving the potential  $V_s + V_e + W_{se}$  and the energy of the electron pair  $E_{\text{tot}} = E_s + E_e$ .

### 2.1. Transmission mode

For (e, 2e) in the transmission mode we consider the experimental set-up that has been employed successfully to map out the electron-momentum spectral density of ordered materials. This technique is known as electron momentum spectroscopy (EMS) [10]. In EMS the two electrons are emitted with high energies ( $E_s \approx E_e \approx E_0/2 \sim 20\text{--}30$  keV) and are detected with wavevectors that correspond to quasielastic (classical) knockout of the valence electron by the incident electron. The free-standing films have a thickness of  $\sim 100\text{--}300$  Å. In this situation the transition operator (2) is well approximated by the plane wave impulse approximation (PWIA), i.e. it reduces to

$$T_{(e,2e)} \approx W_{se} + W_{se}G_{(se)}^+(E_{\text{tot}})W_{se}, \quad (3)$$

where  $G_{(se)}^+(E_{\text{tot}})$  is the two-electron propagator in the potential  $W_{se}$ . The screening of the electron–electron interaction by the surrounding medium is negligible, because the momentum and energy transfer is huge (with respect to the Fermi values). Hence  $W_{se}$  is a bare Coulomb potential. In the case of unpolarized electrons we deduce from (1) and (3)

$$\frac{d\sigma}{dE_s dE_e d\Omega_s d\Omega_e} = \frac{k_s k_e}{(2\pi)^3 k_0} \left( \frac{d\sigma}{d\Omega} \right)_{ee} A^-(\mathbf{k}, \varepsilon), \quad (4)$$

where  $\left( \frac{d\sigma}{d\Omega} \right)_{ee}$  is the Mott scattering cross section that includes the effects of exchange between the colliding electrons. The quantity

$$A^-(\mathbf{k}, \varepsilon) = \sum_{i_{\text{occ}}} |\langle \mathbf{k} | i \rangle|^2 \delta(\varepsilon - \varepsilon_i) \quad (5)$$

is the spectral function of the hole with the wavevector  $\mathbf{k} = \mathbf{k}_e + \mathbf{k}_s - \mathbf{k}_0$  and the energy  $\varepsilon = E_{\text{tot}} - E_0$ . The spectral function (5) contains all relevant information on the (spin-averaged) electronic structure of the sample. Since  $\mathbf{k}$ ,  $\varepsilon$  and  $d\sigma/dE_s dE_e d\Omega_s d\Omega_e$  are determined experimentally one can deduce from the experiment  $A^-(\mathbf{k}, \varepsilon)$  according to (4). This fact is valid irrespective of the nature of the target.

### 2.2. Reflection mode

In the case of (e, 2e) in the reflection mode and at moderate electron energies, we treat (2) only to a first order in the electron–electron interaction  $W_{se}$ . This approximation is equivalent to the distorted wave Born approximation (DWBA). To validate this procedure we choose the kinematics such that  $E_0 \gg \varepsilon_F, \Delta E$  ( $\Delta E \equiv E_0 - E_s$ ). In this context we note that the electron–electron interaction in solids is short-ranged due to the screening and hence a perturbative (Born series) treatment is appropriate. The DWBA transition operator is

$$T_{(e,2e)} \approx [1 + (V_s + V_e)G_{(s,e)}^+(E_{\text{tot}})]W_{se}[1 + G_{(s,e)}^+(E_{\text{tot}})V_s], \quad (6)$$

where  $G_{(s,e)}^+$  is the two-electron Green operator involving the potential  $V_s + V_e$ . Furthermore, as in the kinematical approximation employed in the theory of low-energy electron diffraction (LEED) [17], we account only for a single scattering off the multi-centre potential  $V_s$ . Thus (6) reduces to

$$T_{(e,2e)} = (1 + V_e G_e^+)(V_s g_s^{(0)+} W_{se} + W_{se} g_0^{(0)+} V_s), \quad (7)$$

where  $G_e^+$  is the propagator of the ejected electron involving the potential  $V_e$ . Furthermore,  $g_s^{(0)}$  and  $g_0^{(0)}$  are the free propagators at energies  $E_s$  and  $E_0$ , respectively. Refraction of the electrons at the surface and the damping inside the surface are accounted for by the use of renormalized propagators  $g_s$  and  $g_0$  instead of  $g_s^{(0)}$  and  $g_0^{(0)}$  in (7).

For the evaluation of (1) it is advantageous to couple the spins of the electrons to a total electron-pair spin  $S$ . As the transition operator (7) does not contain spin-flip terms, the sum over the spin projections in (1) is an average of the cross section over the singlet ( $S = 0$ ) and the triplet ( $S = 1$ ) channels [18] and the basic quantity from which the (e, 2e) cross section is evaluated is

$$\frac{d\sigma}{dE_s dE_e d\Omega_s d\Omega_e} = \frac{k_s k_e}{(2\pi)^5 k_0} \sum_{i_{occ}} |\langle \chi_{k_e} | M(\mathbf{k}_s, \mathbf{k}_0) | \chi_i \rangle|^2 \delta(\varepsilon - \varepsilon_i). \quad (8)$$

Here  $|\chi_{k_e}\rangle = (1 + G_e^- V_e) |k_e\rangle$  is the time-reversed scattering state of the ejected electron subject to the potential  $V_e$  and  $|\chi_i\rangle$  is the state of the bound electron. The effective one-electron transition operator is

$$M(\mathbf{k}_s, \mathbf{k}_0) = \langle \mathbf{k}_s | V_s g_s^+ W_{se} + W_{se} g_0^+ V_s | \mathbf{k}_0 \rangle. \quad (9)$$

### 3. Configurational average of the cross section

For simplicity we consider a substitutionally disordered binary alloy  $A_x B_{1-x}$  consisting of two components A and B with concentration  $c_A = x$  and  $c_B = 1 - x$ . We assume full randomness ( $c_A + c_B = 1$ ) and neglect any sort of statistical correlation in the occupation of the lattice sites. Furthermore, we employ the single-site approximation discarding local environment effects [14, 15]. Thus, the lattice potential  $V_{s(e)}$  is expressed as a sum of muffin-tin potential functions  $V_{s(e)}^j$  located at sites  $\mathbf{R}_j$ , i.e.  $V_{s(e)} = \sum_j V_{s(e)}^j$ . Introducing the occupation indices  $\xi^j$  (where the random numbers  $\xi^j = 1$  if the site  $j$  is occupied by the atom of type A and  $\xi^j = 0$  if  $j$  is occupied by atom B), the single-site potential is

$$V_{s(e)}^j = \xi^j V_{s(e)}^{jA} + (1 - \xi^j) V_{s(e)}^{jB}. \quad (10)$$

The configurational average  $\langle \xi^j \rangle$  of  $\xi^j$  is deduced from the probability for the atom A to occupy the site  $j$ , i.e.,  $\langle \xi^j \rangle = x$  (hereafter we use the angle brackets  $\langle \cdot \cdot \rangle$  for configurationally averaged quantities).

#### 3.1. Transmission mode

To obtain the configurational average of the (e, 2e) cross section in the transmission mode, as given by (4) we note that the Mott cross section does not depend on the space configuration of the atoms. Hence we deduce that

$$\left\langle \frac{d\sigma}{dE_s dE_e \Omega_s d\Omega_e} \right\rangle = \frac{k_s k_e}{(2\pi)^3 k_0} \left( \frac{d\sigma}{d\Omega} \right)_{ee} \langle A^-(\mathbf{k}, \varepsilon) \rangle. \quad (11)$$

Thus, the (e, 2e) cross section under EMS conditions delivers direct information on the spectral function  $\langle A^-(\mathbf{k}, \varepsilon) \rangle$  of disordered systems. We recall that both  $\mathbf{k}$  and  $\varepsilon$  are measured by an

EMS experiment and hence  $\langle A^-(\mathbf{k}, \varepsilon) \rangle$  can be mapped out in complete detail. This confirms a long-standing expectation that the EMS is most suitable for the study of disordered systems where the lack of translational symmetry hinders a determination of the  $\mathbf{k}$  dependence of  $\langle A^-(\mathbf{k}, \varepsilon) \rangle$  via ultraviolet photoemission experiments (the UV photon transfers energy but no momentum to the target).

### 3.2. Reflection mode

For the calculation of the configurational average of the (e, 2e) cross section in the reflection mode (equation (8)) the matrix element (9) is written as a sum over the lattice sites:

$$M(\mathbf{k}_s, \mathbf{k}_0) = \sum_j M_j(\mathbf{k}_s, \mathbf{k}_0), \quad \text{where } M_j(\mathbf{k}_s, \mathbf{k}_0) = \langle \mathbf{k}_s | V_s^j g_s^+ W_{se} + W_{se} g_0^+ V_s^j | \mathbf{k}_0 \rangle. \quad (12)$$

From equation (10) it follows that  $M_j(\mathbf{k}_s, \mathbf{k}_0) = \xi^j M_{jA}(\mathbf{k}_s, \mathbf{k}_0) + (1 - \xi^j) M_{jB}(\mathbf{k}_s, \mathbf{k}_0)$ . Substitution of (12) into (8) yields

$$\frac{d\sigma}{dE_s dE_e d\Omega_s d\Omega_e} = \frac{k_s k_e}{(2\pi)^5 k_0} \sum_{jj'} \langle \chi_{k_e} | M_j(\mathbf{k}_s, \mathbf{k}_0) A^-(\varepsilon) M_{j'}^+(\mathbf{k}_s, \mathbf{k}_0) | \chi_{k_e} \rangle, \quad (13)$$

where the one-electron spectral function is given as

$$A^-(\varepsilon) = \sum_{i_{occ}} |\chi_i\rangle \langle \chi_i| \delta(\varepsilon - \varepsilon_i). \quad (14)$$

Performing the configurational average of (13) we decouple the on-site quantities related to the different electrons, i.e. we neglect all two-electron on-site correlated terms in the configurational average and obtain

$$\left\langle \frac{d\sigma}{dE_s dE_e d\Omega_s d\Omega_e} \right\rangle = \left\langle \frac{d\sigma^{\text{coh}}}{dE_s dE_e d\Omega_s d\Omega_e} \right\rangle + \left\langle \frac{d\sigma^{\text{incoh}}}{dE_s dE_e d\Omega_s d\Omega_e} \right\rangle. \quad (15)$$

The terms

$$\left\langle \frac{d\sigma^{\text{coh}}}{dE_s dE_e d\Omega_s d\Omega_e} \right\rangle = \frac{k_s k_e}{(2\pi)^5 k_0} \sum_{jj'} \langle \langle \chi_{k_e} | \langle M_j(\mathbf{k}_s, \mathbf{k}_0) \rangle A^-(\varepsilon) \langle M_{j'}^+(\mathbf{k}_s, \mathbf{k}_0) \rangle | \chi_{k_e} \rangle \rangle \quad (16)$$

and

$$\left\langle \frac{d\sigma^{\text{incoh}}}{dE_s dE_e d\Omega_s d\Omega_e} \right\rangle = \frac{k_s k_e}{(2\pi)^5 k_0} \sum_j \left\{ \sum_{\alpha=A,B} c_\alpha \langle \langle \chi_{k_e} | M_{j\alpha}(\mathbf{k}_s, \mathbf{k}_0) A^-(\varepsilon) M_{j\alpha}^+(\mathbf{k}_s, \mathbf{k}_0) | \chi_{k_e} \rangle \rangle - \langle \langle \chi_{k_e} | \langle M_j(\mathbf{k}_s, \mathbf{k}_0) \rangle A^-(\varepsilon) \langle M_j^+(\mathbf{k}_s, \mathbf{k}_0) \rangle | \chi_{k_e} \rangle \rangle \right\} \quad (17)$$

represent the coherent and the incoherent part of the (e, 2e) cross section which originate from the coherent and incoherent backscattering of the fast electron, respectively.

## 4. Results and discussion

Now we present and analyse numerical results for the energy correlation within the electron pair emitted from copper–nickel alloys. The bound electron state is derived from a self-consistent KKR CPA treatment based on the density functional theory within the local density approximation. This method has proved to be adequate for the electronic structure calculations of alloys of transition metals [14]. In the high-energy transmission mode the scattering dynamics is unaffected by disorder (cf equation (11)). In contrast, in the reflection mode we have to account for the influence of disorder on the propagation and the scattering of the

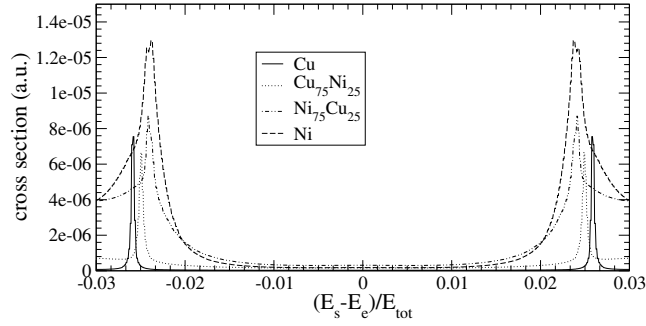


**Figure 2.** The dependence of the  $(e, 2e)$  cross section in the transmission mode on the distribution of the total electron-pair energy  $E_{\text{tot}}$  between the two electrons emitted from the (001) face of a copper–nickel alloy target. The energies are  $E_{\text{tot}} = E_0 - \Phi$  ( $\Phi$  is the work function) and  $E_0 = 50$  keV, i.e. the ejected electron originates from the Fermi level. The polar angles are  $\theta_s = \theta_e = 45^\circ$  with respect to the [001] direction and the wavevectors of all the vacuum electrons are in the (010) plane.

excited electrons (cf equations (16) and (17)). We do this within the VCA [14], which is justified by the rather high (vacuum) electron energies and therefore by the weak scattering of the ejected electrons off the crystal potential<sup>1</sup>.

Figure 2 shows the dependence of the transmission mode  $(e, 2e)$  cross section on the energy sharing of the two electrons for a fixed total energy of the electron pair. We choose an initial electron energy which is typical for EMS ( $E_0 = 50$  keV). The incident projectile momentum is parallel to the [001] direction. The peaks in the energy sharing distributions correspond to the ejection of the bound electron with a Fermi crystal momentum. Their positions are determined by the energy and momentum conservation laws. So that by varying the energy sharing one effectively studies the crystal momentum distribution of the bound electrons at the Fermi energy. For the clean copper sample there is a one-fold Fermi surface and as anticipated there are two narrow peaks in the energy sharing distribution, each of them corresponding to the Fermi surface crossing (the positions of these peaks are essentially symmetrical with respect to the point of equal energy sharing). The wide peaks in the case of clean nickel correspond to the crossing of the three-fold Fermi surface. Thus one can clearly trace in figure 2 the evolution of the Fermi surface from the one-fold in copper to the three-fold in nickel.

In figure 3 the energy sharing distributions are depicted for the case of reflection mode. The initial electron energy is  $E_0 = 200$  eV and the projectile momentum is antiparallel to the [001] direction. For all concentrations there is a structure in the domain  $0.5 > |(E_s - E_e)/E_{\text{tot}}|$  and two wings in the domains  $1 \geq |(E_s - E_e)/E_{\text{tot}}| > 0.5$ . These correspond to the diffraction of the electron pair [6, 19] involving the reciprocal lattice vector  $\mathbf{g}_{\parallel} = (00)$  and  $\pm(11)$ , respectively. In contrast to figure 2 the information on the electronic structure in the energy sharing is overshadowed by the influence of matrix elements. Nevertheless, the evolution of the Fermi surface with the increase of the concentration of nickel in copper can be seen in figure 3. Here the peaks in the energy sharing distribution correspond to a crossing of the Fermi surface in the (001) plane. This follows from the conservation of the surface parallel momentum in (16) as well as from the negligible incoherent contribution (17) in the case of copper–nickel alloys. The latter is due to the small difference between the muffin-tin potentials in copper and nickel that enter (10).

<sup>1</sup> We omit the technical details regarding the numerical evaluation of the  $(e, 2e)$  matrix elements due to the shortage of space.

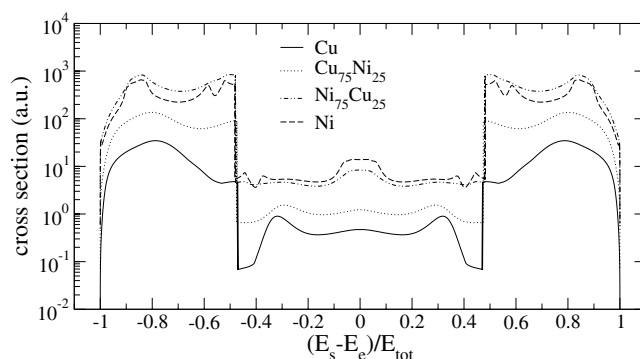


Figure 3. The same as in figure 2 but in the case of reflection mode (cf figure 1(b),  $\theta_s = \theta_e = 45^\circ$ ).

## 5. Conclusion

In this letter we considered theoretically the  $(e, 2e)$  process from binary substitutional alloys. In the transmission mode the  $(e, 2e)$  measurements allow direct access to the alloy's electronic structure. In the reflection mode the  $(e, 2e)$  cross section is determined by the alloy's electronic structure as well as by the collision dynamics averaged over the disorder. Numerical results have been presented and analysed for the case of copper–nickel alloys using the KKR CPA (for ground-state electrons) and VCA (for vacuum electrons). The footprints of the alloy's electronic structure have been identified in the  $(e, 2e)$  cross sections. We have shown that this is generally possible in the case of the high-energy transmission mode and also in the case of the reflection mode, if the difference between the muffin-tin potentials of the alloy's constituents is small enough to neglect the incoherent backscattering of the fast projectile electron.

## References

- [1] Ibach H and Mills DL 1982 *Electron Energy Loss Spectroscopy and Surface Vibrations* (New York: Academic)
- [2] Iacobucci S, Marassi L, Camilloni R, Nannarone S and Stefani G 1995 *Phys. Rev. B* **51** 10252
- [3] Vos M and McCarthy I E 1995 *J. Electron Spectrosc. Relat. Phenom.* **74** 15
- [4] Vos M and Weigold E 1995 *Rev. Mod. Phys.* **67** 713
- [5] Artamonov O M, Samarin S N and Kirschner J 1997 *Appl. Phys. A* **65** 535
- [6] Berakdar J, Samarin S N, Herrmann R and Kirschner J 1998 *Phys. Rev. Lett.* **81** 3535
- [7] Feder R, Gollisch H, Meinert D, Scheunemann T, Artamonov O M, Samarin S N and Kirschner J 1998 *Phys. Rev. B* **58** 16418
- [8] Kheifets A S, Iacobucci S, Ruocco A, Camilioni R and Stefani G 1998 *Phys. Rev. B* **57** 7360
- [9] Gollisch H, Scheunemann T and Feder R 2001 *Solid State Commun.* **117** 691
- [10] Weigold E and Vos M 2001 *Many Particle Spectroscopy of Atoms, Molecules, Clusters, and Surfaces* ed J Berakdar and J Kirschner (New York: Kluwer) p 417
- [11] Berakdar J and Das M P 1997 *Phys. Rev. A* **56** 1403
- [12] Morozov A, Berakdar J, Samarin S N, Hillebrecht F U and Kirschner J 2002 *Phys. Rev. B* **65** 104425
- [13] Canney S A, Vos M, Kheifets A S, Guo X, McCarthy I E and Weigold E 1997 *Surf. Sci.* **382** 241
- [14] Gonis A 2000 *Theoretical Materials Science: Tracing the Electronic Origins of Materials Behaviour* (Warrendale, PA: Materials Research Society)
- [15] Turek I, Drchal V, Kudrnovský J, Šob M and Weinberger P 1997 *Electronic Structure of Disordered Alloys, Surfaces, and Interfaces* (Boston, MA: Kluwer)
- [16] Faulkner J S and Stocks G M 1980 *Phys. Rev. B* **21** 3222
- [17] Van Hove M A, Weinberg W H and Chan C-M 1986 *Low-Energy Electron Diffraction. Experiment, Theory and Surface Structure Determination* (Berlin: Springer)
- [18] Berakdar J 1999 *Phys. Rev. Lett.* **83** 5150
- [19] Samarin S, Berakdar J, Artamonov O, Schwabe H and Kirschner J 2000 *Surf. Sci.* **470** 141